Rheological characterisation of concentrated domestic slurry

Thota Radhakrishnan, A. K.; van Lier, J. B.; Clemens, F. H.L.R.

DOI
10.1016/j.watres.2018.04.064

Publication date
2018

Document Version
Final published version

Published in
Water Research

Water Research 141 (2018) 235–250

Contents lists available at ScienceDirect

Water Research

journal homepage: www.elsevier.com/locate/watres

Rheological characterisation of concentrated domestic slurry

A.K. Thota Radhakrishnan [a, *], J.B. van Lier [a], F.H.L.R. Clemens [a, b]

[a] Delft University of Technology, Civil Engineering and Geosciences, Department of Water Management, P.O. Box 5, 2600 AA Delft, The Netherlands
[b] Deltares, Department of Industrial Hydrodynamics, P.O. Box 177, 2600 MH Delft, The Netherlands

ARTICLE INFO

Article history:
Received 24 January 2018
Received in revised form
23 April 2018
Accepted 27 April 2018
Available online 3 May 2018

Keywords:
Rheology
Concentrated domestic slurry
Novel sanitation
Parameter estimation
Error-analysis
Concentration and temperature influence

ABSTRACT

The much over-looked element in new sanitation, the transport systems which bridge the source and treatment facilities, is the focus of this study. The knowledge of rheological properties of concentrated domestic slurry is essential for the design of the waste collection and transport systems. To investigate these properties, samples were collected from a pilot sanitation system in the Netherlands. Two types of slurries were examined: black water (consisting of human faecal waste, urine, and flushed water from vacuum toilets) and black water with ground kitchen waste. Rheograms of these slurries were obtained using a narrow gap rotating rheometer and modelled using a Herschel-Bulkley model. The effect of concentration on the slurry are described through the changes in the parameters of the Herschel-Bulkley model. A detailed method is proposed on estimating the parameters for the rheological models. For the black water, yield stress and consistency index follow an increasing power law with the concentration and the behaviour index follows a decreasing power law. The influence of temperature on the viscosity of the slurry is described using an Arrhenius type relation. The viscosity of black water decreases with temperature. As for the black water mixed with ground kitchen waste, it is found that the viscosity increases with concentration and decreases with temperature. The viscosity of black-water with ground kitchen waste is found to be higher than that of black water, which can be attributed to the presence of larger particles in the slurry.

1. Introduction

Critical evaluation of our current sanitation system has led to the introduction of a new sanitation paradigm (see e.g. Kujawa-Roeleveld et al., 2006; Tervahauta et al., 2013; Zeeman et al., 2008). The new paradigm is based on source separation of the waste (as depicted in Fig. 1) and minimizing the use of water for transport. This source separated waste consists primarily of faecal matter from vacuum toilets, toilet paper and grinded kitchen waste arising from the use of food waste disposers. These domestic waste streams are subsequently treated with the objective to minimize energy use during treatment while maximizing the recovery of resources present in the wastewater, namely: bio-energy (generated from the anaerobic transformation of organic material), nutrients (nitrogen, phosphorus, potassium and sulphur), and water.

Although significant advancements have been made with respect to treatment processes in the new sanitation systems, the collection and transport aspects of the wastewater bridging source (e.g., households or industrial complexes) and treatment facilities, have been grossly neglected. Transport of the collected slurries is of particular interest when the new paradigm will be applied in a large scale. For any further development of the 'source-separated sanitation' approach, both transport and treatment are inseparable parts of the entire sanitation system and requires full assessment in order to evaluate its potentials for future waste handling (Larsen et al., 2009).

In order to design and operate a transport system for source-separated **C**oncentrated **D**omestic **S**lurry (CDS) composed of **B**lack **W**ater (BlW) that consists of human faecal waste, urine, and flushed water from vacuum toilets and **G**rinded **K**itchen **W**aste (GKW), detailed knowledge about the physical properties of transported liquid, particularly its rheology, is essential (Chilton et al., 1996; Slatter and Thomas, 1995; Thomas and Wilson, 1987). It has been shown that even the basic aspects of a pipeline design, for example the expected flow regime (laminar or turbulent) and pressure drop, can be misjudged without a rigorous understanding of the rheology (Eshtiaghi et al., 2012).

Food waste disposers (FWD) are an integral part of the new

* Corresponding author.
E-mail address: a.k.thotaradhakrishnan@tudelft.nl (A.K. Thota Radhakrishnan).

https://doi.org/10.1016/j.watres.2018.04.064

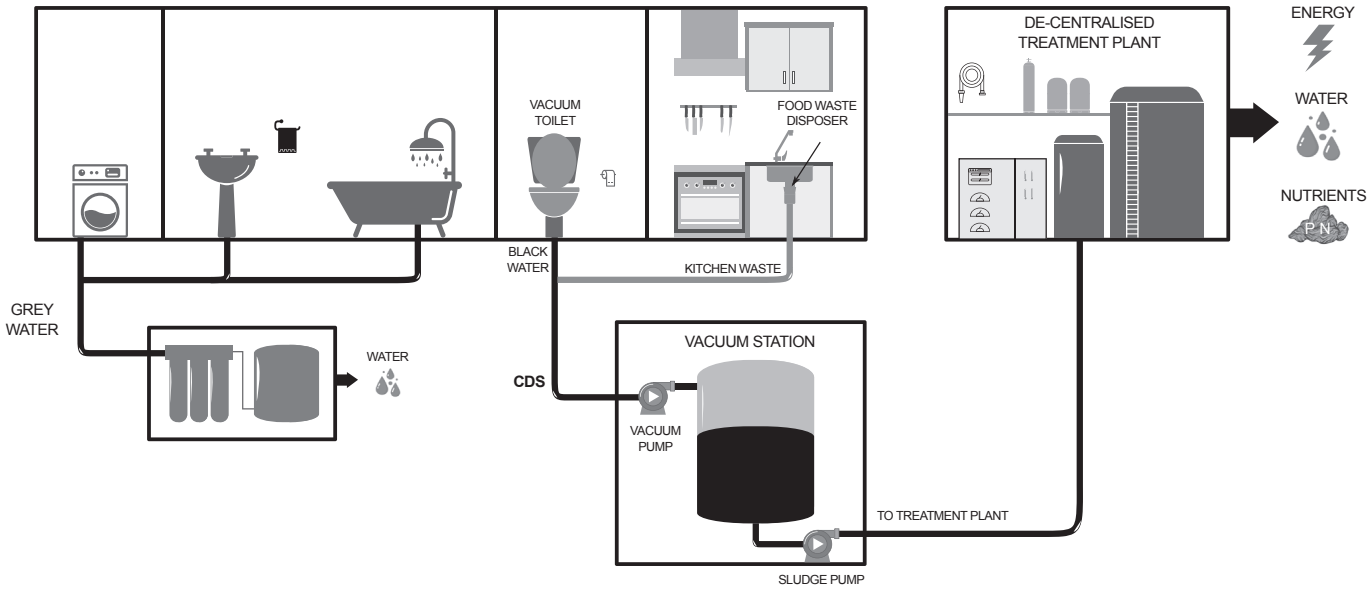

Fig. 1. Schematic representtion of a sanitation system according to decentralised sanitation and reuse concept.

sanitation paradigm. They macerate the kitchen food waste and dispose them into the sewer system. FWDs have been identified by many researchers as an effective domestic food waste management strategy (Iacovidou et al., 2012a; Lundie and Peters, 2005; Nakakubo et al., 2012). They may increase resource recovery in particular when connected to an anaerobic digester (Braun and Wellinger, 2003; Iacovidou et al., 2012b). Although many researchers have recommended FWDs, they have also indicated that for a large scale implementation or for higher market penetration, the implications of FWDs environment and conventional sewer system with respect to its transportation need to be examined, an overview of this can be found in (Iacovidou et al., 2012a). Therefore, it is only important that the transport of these GKW is assessed.

1.1. Current state-of-art

The state of the art on the solids content of wastewater in traditional sewer systems is summarised in the book *Solids in sewers* (Ashley et al., 2005). Although it provides great details regarding the origin and physio-chemical properties of the wastewater, rheological properties have not been characterised. It is common that a viscosity close to pure water is considered for the design of traditional sewer systems (Hager, 2010). However, CDS is much less diluted compared to the traditional domestic waste (Tervahauta et al., 2013); therefore, it is expected to have a considerably larger (apparent) viscosity.

Many studies have investigated the rheological behaviour of the primary, secondary, and aerobic/anaerobic digested sludge in treatment plants as summarised in (Eshtiaghi et al., 2013a, b; Ratkovich et al., 2013). It was concluded that the sludge is a non-Newtonian fluid showing a shear-thinning thixotropic behaviour. On the existence of the yield stress, no agreement was found. However, the obtained results are not directly applicable to the CDS, because primary and secondary sludge do not represent fresh faecal sludge and they undergo different treatments that change the structure of suspended organic matter present in the slurry. A study on fresh faecal sludge by (Woolley et al., 2014), is the only available literature on this. Unfortunately, their study doesn't give much information on procedure and collection to make the study useful for analysis. The inclusion of waste from FWDs also increases the flow complexity of these slurries. Apparently, the rheological knowledge of sludge in treatment plants cannot be directly used to reliably estimate the rheological properties of CDS; therefore, proper measurement needs to be conducted to investigate these properties. The current work presents measurements that were carried out to characterise the rheological properties of CDS. The

Table 1
Summary of investigated concentrations.

Slurry 1: Faecal		Slurry 2: Faecal + GKW	
Concentration (% TSS wt./wt.)	Concentrating method	Concentration (% TSS wt./wt.)	Concentrating method
11.2	Centrifugation	3	Gravity
10	Centrifugation	2.6	Gravity
7.2	Gravity	2.1	Gravity
5	Gravity	1.8	Gravity
3.9	Gravity	1.2	Gravity
3.2	Gravity	1	Gravity
2.6	Gravity	0.8	Gravity
1.8	Gravity		
1.4	Gravity		
0.7	Gravity		
0.4	Gravity		

influence of two parameters, namely temperature and concentration is examined. Based on the outcome of the measurement, the fluid models that describe the rheological behaviour of CDS are introduced. Also, the inclusion of GKW is accessed from a rheological aspect of these slurries. A summary of the investigated concentration is presented in Table 1.

2. Method and material

2.1. CDS sample

Two samples of domestic slurry were collected. ***Slurry 1***, BlW consisting of human faecal waste, toilet paper and flushed water was collected from a vacuum collection experimental facility in the building of DeSaH B.V. in Sneek, the Netherlands. The vacuum collection system consists of a urine separation vacuum toilet connected to a collection tank through a vacuum pump. The vacuum pump is fitted with a cutter upstream (Fig. 2b) to cut the incoming waste. ***Slurry 2***, BlW with GKW was collected from the housing project "Noorderhoek" consisting of 215 houses in Sneek, Netherlands. These houses have source separation implemented in them along with vacuum toilets and food (kitchen) waste disposers. Slurry 2 is collected from a collection tank as shown in Fig. 2a. It has to be noted that prior to the collection, the CDS passes through a cutter pump (as shown in Fig. 2b) which transfers it from a vacuum tank to the collection tank (as schematized in Fig. 2a). In some vacuum stations, the waste is directly transferred from the vacuum tank to the treatment plant by sewage pumps without any intermediate collection tanks. In such configurations, there are cutters installed upstream of the tank to break down the large lumps.

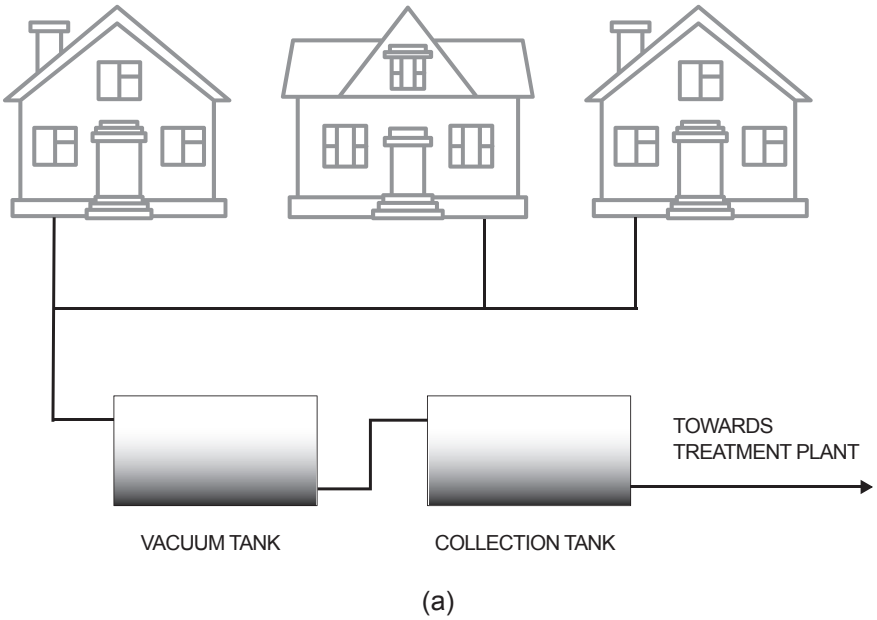

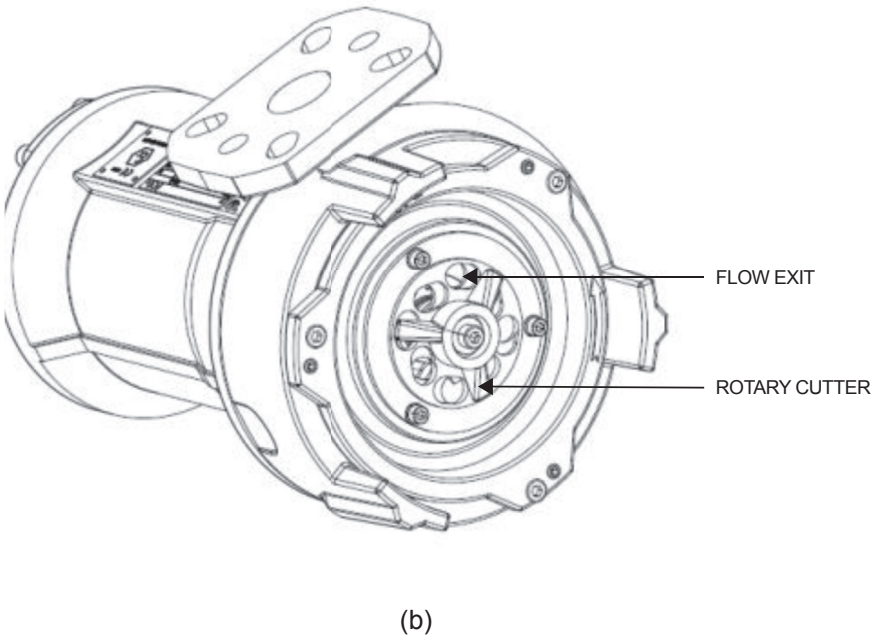

Fig. 2. a) Schematic drawing of a vacuum collection station. b) Cutter pump (submersible disintegrator pump manufactured by Landustrie).

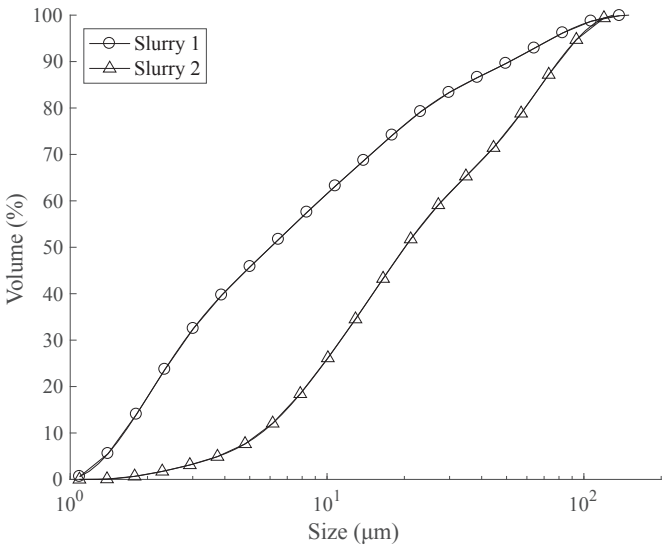

Fig. 3. Cumulative particle size distribution of slurry 1 and slurry 2.

The samples thus collected were immediately transported to the laboratory in a cool box at 4 °C ± 1 °C. The procedure followed the advice for the preservation of wastewater samples given in (Association, 2005) in order to retard biological activity and microbiological decomposition in the samples. In order to preserve the original moisture content and avoid reactions with air, the samples were kept in sealed containers. Once in laboratory, the samples were maintained refrigerated at the same conditions, minimizing changes in the organic compounds during storage until testing.

To obtain slurry 1 as fresh as possible, the collection tank was emptied and cleaned a day before sampling and the toilets were connected to the tank at the morning of collection day. In addition, to obtain a good representative sample, slurry 2 was collected during the evening, at the peak of usage of the toilets and food waste disposers. The maximum retention time of the samples was five hours at the room temperature. The samples were tested within 3 days of its collection.

2.1.1. Sample preparation

Existence of large particles in a sample puts a constraint on the geometry of the rotational rheometer. In order to ensure a continuum description of the flow, a gap size to a maximum particle size ratio should be 10 or more to guarantee a shear flow (Van Wazer, 1963). To ensure this, both slurries 1 and 2 were screened by passing through a mesh with opening size of 2 mm for removing coarse particles which only comprise a negligible portion of the total solids in the wastes. Hereafter, the samples were sieved using a mesh of opening size of 0.125 mm which was carefully chosen to minimise the material loss during sieving and to maximise the particle to rheometer gap ratio. Through this procedure, the total suspended solids (TSS) that is lost from sieving is between 10% and 20%. This low percentage of loss can be attributed to the presence of a grinder pump (as shown in Fig. 2b), which transfers the CDS from the vacuum tank to the collection tank. The cumulative particle size distribution for both slurries 1 and 2 presented in Fig. 3, is used to calculate the minimum gap size. As a standard, the minimum gap size must be 10 times the D90 (representative particle size) of the slurry. The D90 for slurry 1 is 51μm and for slurry 2 is 80μm. Therefore, a gap size of 800μm would be satisfactory for both slurries.

The TSS upon collection of slurry 1 was 2.6% TSS (wt./wt.) and slurry 2 was 1.8% TSS (wt./wt.). The samples were then concentrated to study its rheology at various concentrations. Using gravity settling slurry 1 was concentrated to 7.2% TSS (wt./wt.) and slurry 2−3% TSS (wt./wt.). The obtained supernatant of each sample was respectively used to dilute the sample to obtain different concentrations. Slurry 1 was further concentrated to 11.2% TSS (wt./wt.) by centrifugation at 10 G for 1 min, and then diluted to 10% using the supernatant. The centrifugation procedure was adapted to make sure that the settled particles were suspended upon gentle shaking. This was deemed necessary to ensure that the original flocs were maintained with minimal changes.

2.2. Rheometry

Commonly used rheometers, capable of measuring fundamental rheological properties of sludge, are placed into two general categories (Eshtiaghi et al., 2013a, b): rotational rheometer and capillary rheometers. Advantages and disadvantages of each category have been described in (Eshtiaghi et al., 2013a, b; Seyssiecq et al., 2003; Slatter, 1997). The rotational rheometer has become widely accepted in recent years as the most common class of rheometer utilised in sludge rheology (Eshtiaghi et al., 2013a, b), and is also used in this study.

The rheology measurements were performed with a MCR302 instrument from Anton Paar (Graz, Austria) equipped with a standard cup and bob (cup diameter: 29.29 mm, bob diameter: 27 mm, bob length: 40.5 mm). This geometry has a gap size 1145μm, satisfying the minimum required gap size mentioned in section 2.1. A Peltier temperature control system was used to set and maintain the temperature with an accuracy of ±0.1 °C. The rheology was measured at 10 °C, 20 °C, 30 °C and 40 °C for each concentration to determine the influence of temperature. To avoid evaporation during the measurements, a lid was installed on the cup to cover the sample. It is suggested that for slurries of this nature, a pre-shear is required to erase material memory and to have similar initial conditions for all samples (Baudez et al., 2013, 2011). Therefore, for each investigation the sample was pre-sheared for 5 min at a shear-rate of 1000 s^{-1}, and then left to rest for 5 min, these conditions were found suitably to reproduce results. The rheogram for each investigation was obtained by a step-wise shear ramp-up procedure, and recording the steady state shear-stress for every set shear-rate. Through the step-wise shear ramp-up the inertia of the equipment is avoided by waiting for steady state at each measurement point (Baroutian et al., 2013). This ensures that the inertia of the fluid and the equipment is eliminated. A ramp-down procedure is avoided as it would considerably include the inertia of the fluid; as the fluid that is rotating at a higher angular velocity is slowed down which causes a delay in reaching steady-state. The shear-rate range was so determined to avoid the occurrence of secondary flows (Thota Radhakrishnan et al., 2015). At the end of every test, the used sample was discarded and a fresh sample was used for the next test.

2.3. Rheological model

Rheological models are an empirical representation of the obtained rheogram (graphical representation of shear-stress vs. shear-rate). For design purposes, the rheological models are used rather than the rheograms. As rheology is the single most important representation of the hydrodynamic behaviour, any discrepancy with the rheological prediction using the model would lead to poor process design as rheology is usually extrapolated for turbulent flow predictions (Slatter, 1997). Therefore, the choice of the rheological model is critical in this aspect. The models used

commonly are:

$\tau = \mu_N \dot{\gamma}$	the Newtonian model that represents a linear relationship between shear-stress and shear-rate.	Equation 1
$\tau = K_O \dot{\gamma}^{n_O}$	the Ostwald model that represents a power law relationship between the shear-stress and shear-rate showing a shear thinning behaviour with $n < 1$.	Equation 2
$\tau = \tau_{yB} + \mu_B \dot{\gamma}$	the Bingham model represents a fluid with a yield stress. The yield stress is the minimum shear-stress required for the fluid to start flowing.	Equation 3
$\tau = \tau_{yHB} + K_{HB} \dot{\gamma}^{n_{HB}}$	the Herschel-Bulkley (HB) model is used to represent a shear-thinning fluid with a yield stress.	Equation 4
$\tau = \tau_{yCHB} + \mu_{CHB} \dot{\gamma} + K_{CHB} \dot{\gamma}^{n_{CHB}}$	the combined Herschel-Bulkley (CHB) used by Baudez (Baudez et al., 2013, 2011) represents well the linear shear-thinning behaviour at high shear-rates giving a constant high-shear viscosity. It is merely a HB model coupled with a Newtonian model.	Equation 5

Elaborate reviews on the models available have been already provided in articles by Seyssiecq et al. (2003) and Eshtiaghi et al. (2013a, b).

2.4. Statistical assessment

To access the predictive capability of the selected rheological models mentioned in section 2.3 the following statistical descriptors are used. The root mean square error (RMSE) measures the overall accuracy of the model. The squared sum error SSR measures the square of the absolute deviation of the model.

$$RMSE = \sqrt{\frac{\sum_{i=1}^{n} (\tau_i - \widehat{\tau}_i)^2}{n}} \tag{6}$$

$$SSR = \sum_{i=1}^{n} (\tau_i - \widehat{\tau}_i)^2 \tag{7}$$

2.5. Parameter estimation

The goal of the parameter estimation step is to determine a unique set of model parameters for the obtained rheometric data (Ratkovich et al., 2013). This is done using optimisation algorithms by minimizing the square of the residuals between the model and the experimental data. Although this step seems straightforward (by using commercially available software), implicit assumptions in the optimization algorithms, violation of boundaries of the model parameters and over parameterization can lead to obtaining parameters that are often not unique or physically meaningless. Care must be taken in estimating these parameters and for this reason two optimization algorithms have been used in the study and shall be detailed below:

2.5.1. Genetic algorithm + Trust Region (GTR)

Minimization of the square of the residuals is a quadratic problem. Most gradient-based optimization algorithms are very sensitive to the initial point and thus obtain only some local minima in the proximity of the initial point. As most rheological models are non-linear, there may exist many local minima. Identifying the most optimal minima (preferably the global minimum) of these satisfying the boundary conditions in place requires the optimization procedure to run many initial points, for which the results of the Genetic Algorithm provide valuable information (i.e. it results in a global map of the location of local minima, which in turn are candidates to be investigated further using some gradient based search algorithm). A Genetic algorithm is one such tool that helps in achieving this in a systematic manner. In this algorithm, an

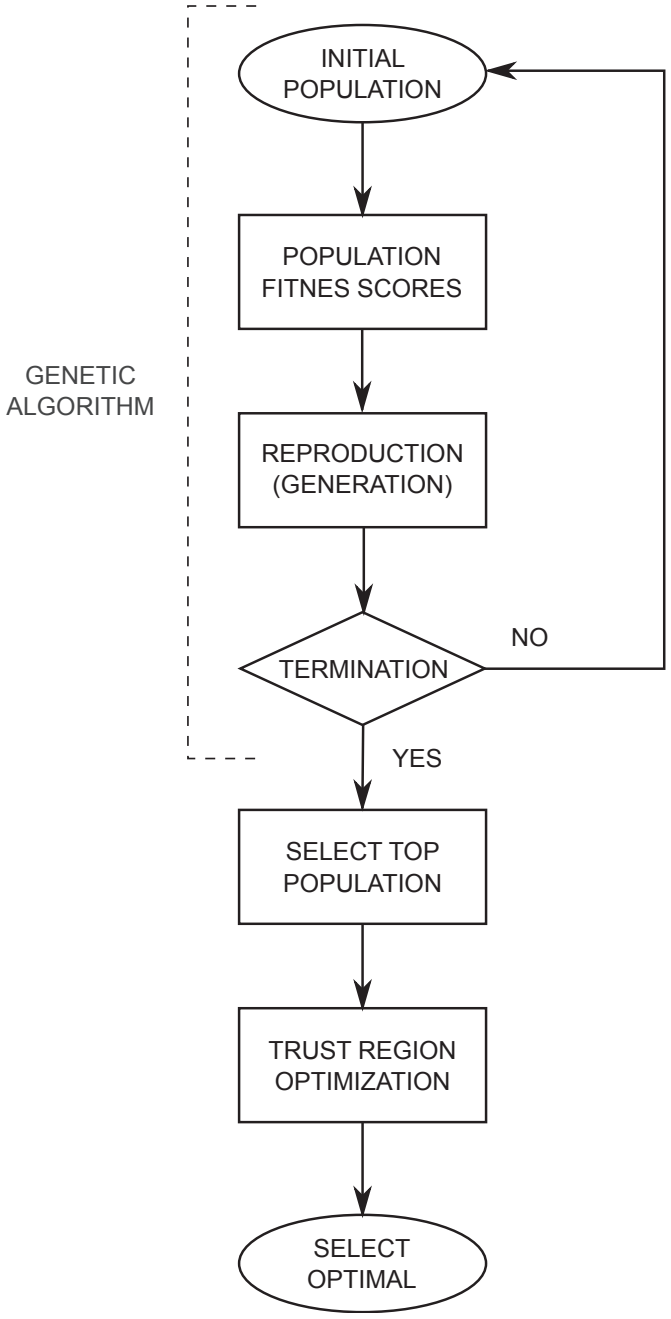

Fig. 4. Genetic algorithm + trust region parameter estimation procedure shown in a flow diagram.

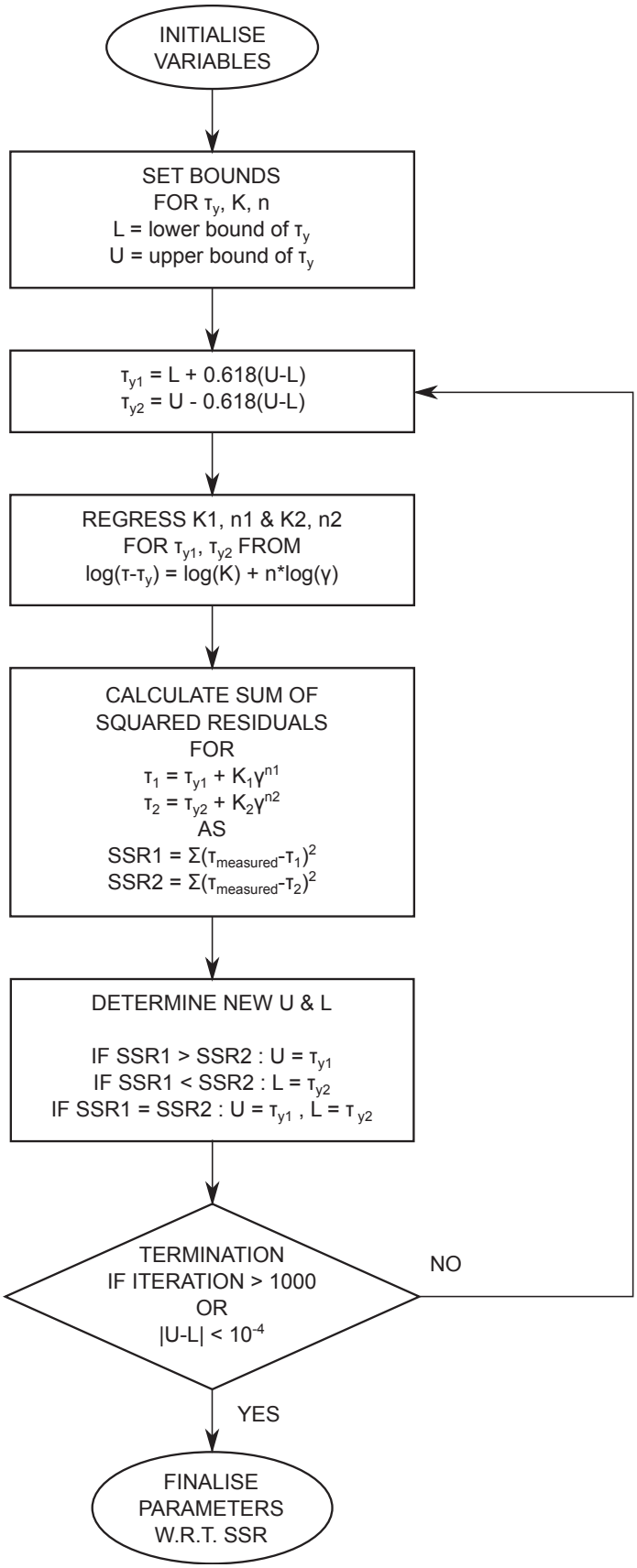

Fig. 5. Golden section search parameter estimation procedure shown in a flow diagram.

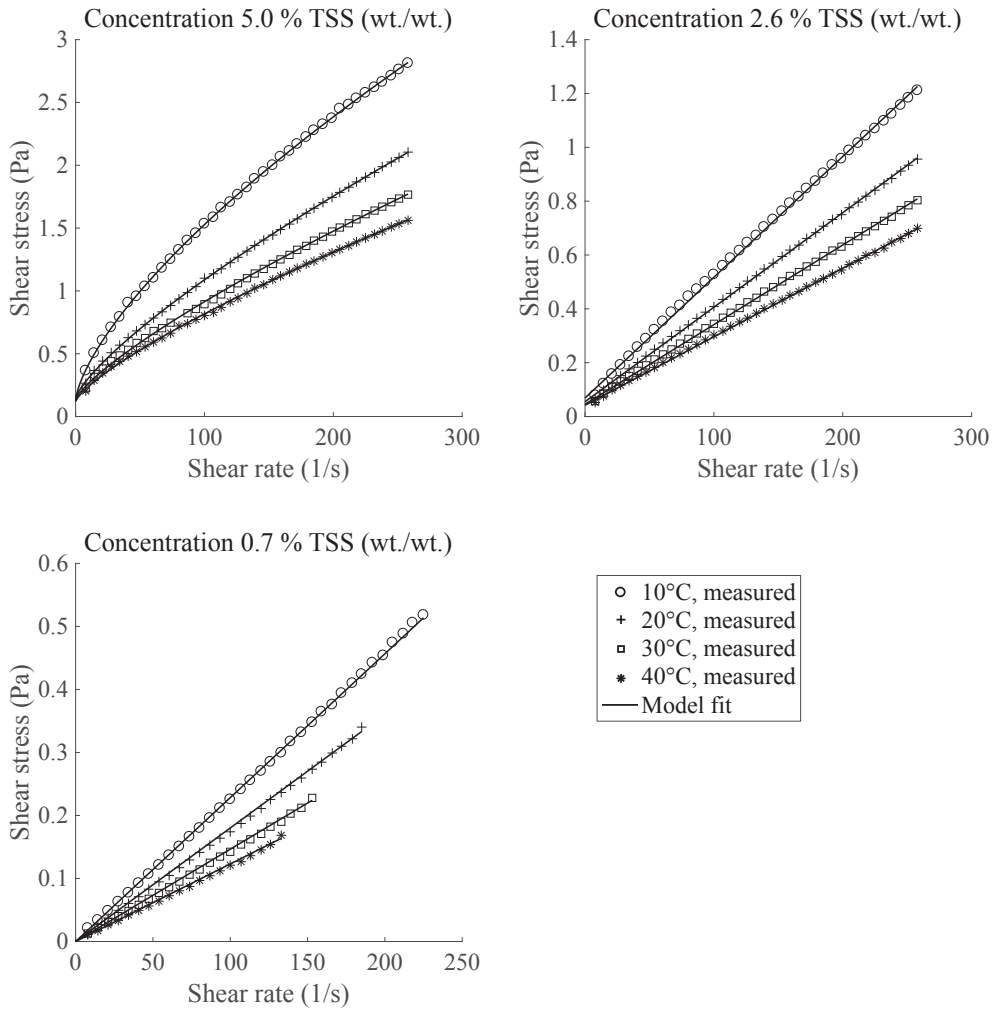

Fig. 6. Representative rheograms for Slurry 1 at various concentrations and temperatures; the respective model used for fitting is indicated in Table 4.

initial population of a random set of parameters (within the boundary specified) is generated. In our case the boundaries depend on the parameters and in general are, $0 < \tau_y$, $0 < K$ and $0 < n < 1$. Using the objective function, the corresponding fitness values for each set of parameters is determined. Using this information, a new generation is produced by applying three genetic operations namely: reproduction, crossover and mutation (Chaudhuri et al., 2006). These operations ensure that a minimum that is found is investigated, and also new sets of parameters are added to avoid being stuck in a local minimum. More information on this approach can be found in (Chaudhuri et al., 2006; Rooki et al., 2012). Each population that is generated is likely to converge to the global minimum. Although a stand-alone genetic algorithm is sufficient for convergence, but to ensure this a gradient-based optimization algorithm is coupled with it. After a number of generations (termination) from the Genetic Algorithm, a part of the population with high scores of fitness value based on the RMSE (Equation (6)) is taken and fed to a gradient-based optimization procedure. A trust region (Byrd et al., 1987) optimization which is a simple gradient based algorithm is used in this case. Hereafter, the parameter set with the lowest RMSE (Equation (6)) is chosen as the optimal solution. This entire algorithm is schematized in Fig. 4. In this study, this algorithm is used in general for all modelling purposes.

2.5.2. Golden section search (GSS)

The golden section search method was proposed by (Ohen and Blick, 1990) for determining model parameters of the Robertson-Stiff fluid model. This numerical scheme was later modified by (Kelessidis et al., 2006) to be used for predicting the parameters for a HB fluid model. In their paper (Kelessidis et al., 2006), the authors demonstrated that the GSS method lead to meaningful and appropriate values for the model parameters. This algorithm is particularly helpful when the parameters are correlated, which is the case with the HB model and will be discussed later. The algorithm essentially de-couples the parameters and reduces the correlation in their estimation. This numerical scheme has been used in this paper and is presented in Fig. 5. In this study, this algorithm is only used to find more accurate solutions for the HB model.

3. Results and discussion

3.1. Rheology

The rheograms for slurry 1 as shown in Fig. 6 (a few representative rheograms) and slurry 2 as shown in Fig. 7 (a few representative rheograms) at various concentrations and temperatures were obtained using the shear-rate ramp up procedure mentioned in section 2.2. For slurry 1 the concentrations ranged between 0.4% and 11.2% TSS (wt./wt.) and for slurry 2 the concentration ranged

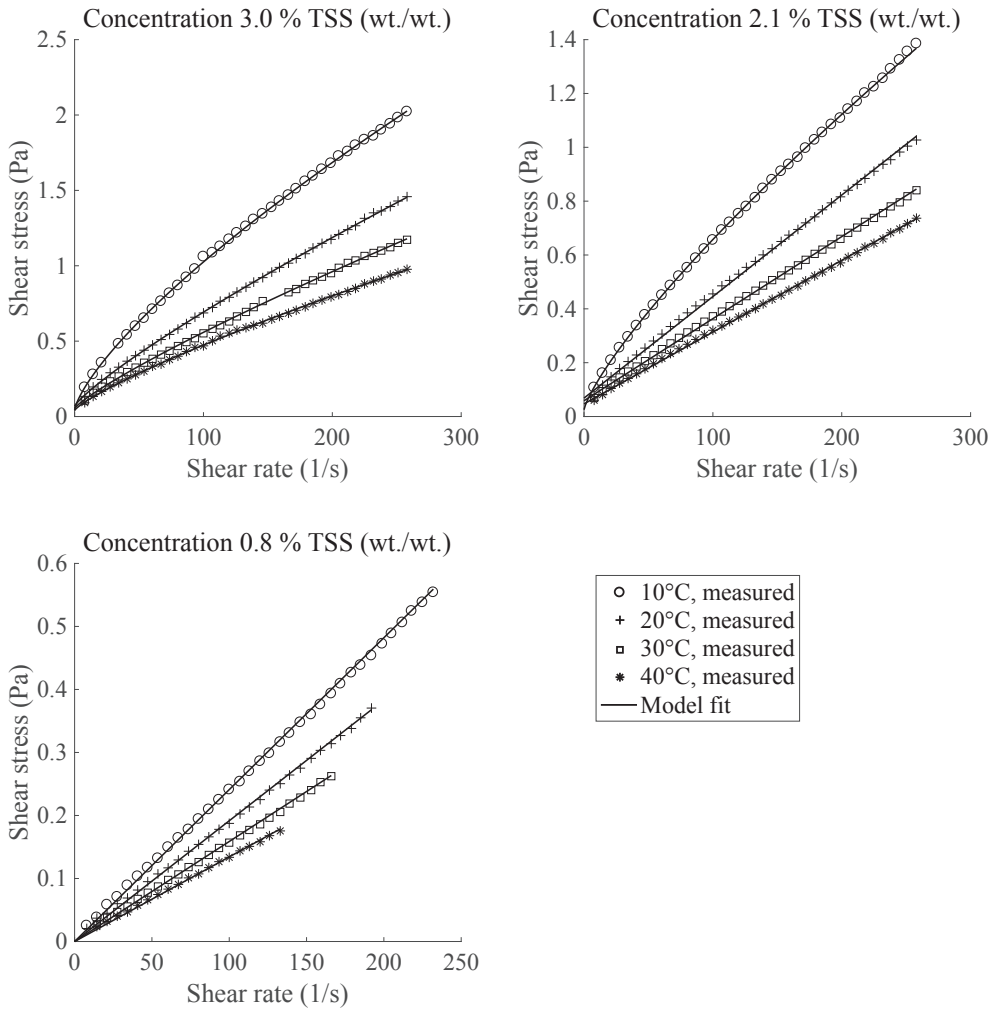

Fig. 7. Representative rheograms for Slurry 2 at various concentrations and temperatures; the respective model used for fitting is indicated in Table 5.

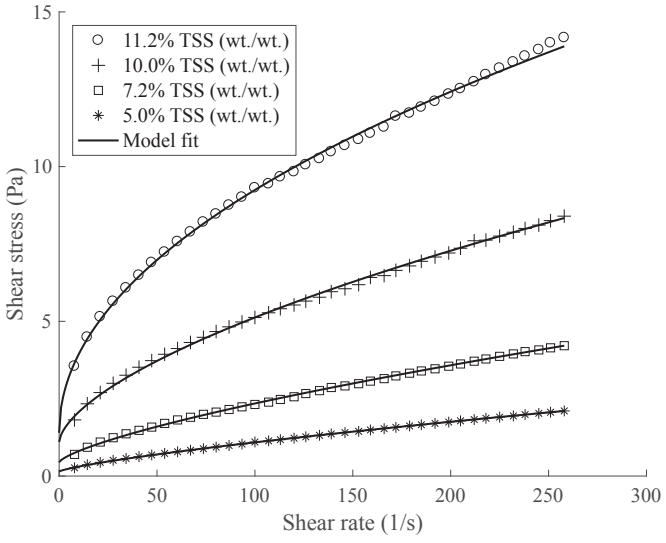

Fig. 8. Rheogram of slurry 1 at various concentration and a fixed temperature of 20 °C; the respective model used for fitting is indicated in Table 4.

between 0.8% and 3.0 %TSS (wt./wt.). For each sample the influence of temperature was evaluated at 10 °C, 20 °C, 30 °C and 40 °C. The steady-state laminar data was used in creating these rheograms. This was ensured by identifying the onset of secondary flows (Thota Radhakrishnan et al., 2015), and removing it from the obtained data. More details on identifying laminar flow and secondary flow along with the range of shear-rates can be found here (Thota Radhakrishnan et al., 2015). This therefore influenced the maximum applicable shear-rate for each concentration and temperature depending on the onset of secondary flows.

From the rheograms, it can be observed that the shear-stress

Table 2
RMSE for the model fit of slurry 1 rheograms at 20 °C.

Concentration	RMSE				
% TSS (wt./wt.)	HB	CHB	Power	Linear	Bingham
11.2	1.25E-02	6.93E-03	3.19E-02	6.16E+00	2.61E-01
10	5.17E-03	2.63E-03	1.77E-02	1.56E+00	6.49E-02
7.2	7.76E-04	5.52E-04	4.78E-03	2.15E-01	9.37E-03
5	4.93E-05	3.47E-05	6.16E-04	2.95E-02	1.74E-03
3.9	9.30E-05	1.44E-05	1.91E-04	7.15E-03	4.42E-04
3.2	1.26E-04	2.70E-05	1.40E-04	3.74E-03	2.74E-04
2.6	1.05E-04	4.28E-05	7.35E-05	8.40E-04	3.36E-05
1.8	1.72E-04	1.92E-05	2.12E-05	5.83E-05	4.38E-06
1.4	3.01E-04	2.18E-05	1.33E-04	8.95E-06	6.59E-06
0.7	8.40E-05	1.15E-05	1.32E-05	1.21E-05	1.16E-05
0.4	2.48E-04	1.83E-05	1.30E-05	1.47E-05	1.46E-05

Table 3
RMSE of the model fit for slurry 2 rheograms at 20 °C.

Concentration	RMSE				
% TSS (wt./wt.)	HB	CHB	Power	Linear	Bingham
3	2.00E-04	1.49E-04	2.69E-04	6.25E-03	3.98E-04
2.6	2.14E-04	2.32E-04	1.25E-04	2.89E-03	2.04E-04
2.1	1.06E-04	8.72E-05	1.04E-04	1.56E-03	8.70E-05
1.8	1.62E-04	2.05E-05	7.67E-05	8.48E-04	3.16E-05
1.2	1.45E-04	4.08E-05	7.31E-05	4.02E-04	2.11E-05
1	2.80E-04	5.80E-05	6.01E-05	2.33E-04	1.44E-05
0.8	5.24E-05	9.07E-06	1.23E-05	1.89E-05	7.08E-06

increases non-linearly with respect to the shear-rate at high TSS concentrations in slurry 1. At low TSS concentration, the shear-stress is a linear function of shear-rate for both slurry 1 and 2. As for the influence of temperature, it is observed that the increase in temperature reduces the shear-stress. This can be attributed to the increase in thermal motion of the molecules and thereby reducing the forces between the molecules resulting in an ease of the flow of the slurry, thus lowering the viscosity.

The influence of increasing the solid content in the slurry can be seen in Fig. 8, which is slurry 1 at various concentrations but at a fixed temperature of 20 °C. The illustration shows an increase in shear-stress with the increase in shear-rate. This observation has also been reported in many other studies (Baroutian et al., 2013). This increase is due to the increase in interactions between the constituent particles present in the slurry. The increase in interactions results in increase in the energy loss, thereby requiring more energy i.e. high shear-stress to keep the slurry in a prescribed motion. As mentioned in (Baroutian et al., 2013), polysaccharides and proteins are likely the determining constituents for the rheological properties of these slurries.

3.2. Rheological modelling

The rheological models described in section 2.3 were used to describe the obtained rheology data. It must be noted that this process of fitting the experimental data to a rheological model is tedious; it requires a priori information and a structured methodology. This is due to the empirical nature of the models that are used to fit the data. In practice a single model is used to fit an entire data set, but this fails due to the correlation between the parameters (Ratkovich et al., 2013). This can be seen from the errors (Fig. 7) from the model fitting using the GTR algorithm to the different models. The model comparison is done using the residuals from the same optimisation algorithm so as to not bias the results. Therefore, based on the RMSE errors from the parameter estimation, the best model is chosen to represent the rheology data. At low concentrations, there is a linear relationship between the shear-stress and shear-rate, but at concentrations >3 %TSS it is observed there exists a non-linear/non-Newtonian relationship.

The yield stress isn't a measured quantity. It is one that is derived as a parameter from the model, essentially extrapolating the obtained rheology data. It is therefore difficult to estimate the true yield stress, and a minimum threshold yield stress of 0.01 Pa is taken for considering its existence. This value is used to determine the appropriate model at low %TSS. From Tables 2 and 3, although the Bingham model fits better at lower %TSS, a linear model is chosen as the yield stress from the Bingham model is < 0.01 Pa. The power law model was the least suitable for all the cases. At higher % TSS, the CHB model used by (Baroutian et al., 2013) is a better fit than that of the HB model. This can entirely be attributed to the increase in the degree of freedom of the optimisation by adding another parameter. But, to further investigate the applicability of the HB and CHB models, the identifiability of their parameters is to be accessed.

To assess the identifiability of the parameters, principal component analysis (PCA) is used. This is done using the Jacobian of the models from Equation (8) and Equation (12). Singular value decomposition of the matrix $\underline{J}^T\underline{J}$ (Equation (17)) gives information about the identifiability of the parameters. The diagonal terms of the matrix Σ is the variance of the parameter combination and the matrix V gives the singular values. Fig. 9 illustrate the singular values of the parameter combination. It can be seen that the CHB model performs poorly as the parameter combinations are co-dependent. This implies that there cannot be a meaningful parameter estimation using this model. But, when accessing the Eigen vectors of the HB model (Fig. 9), it can be seen that the parameter combinations are less co-dependent. Therefore, the HB model is a more relevant model to be used.

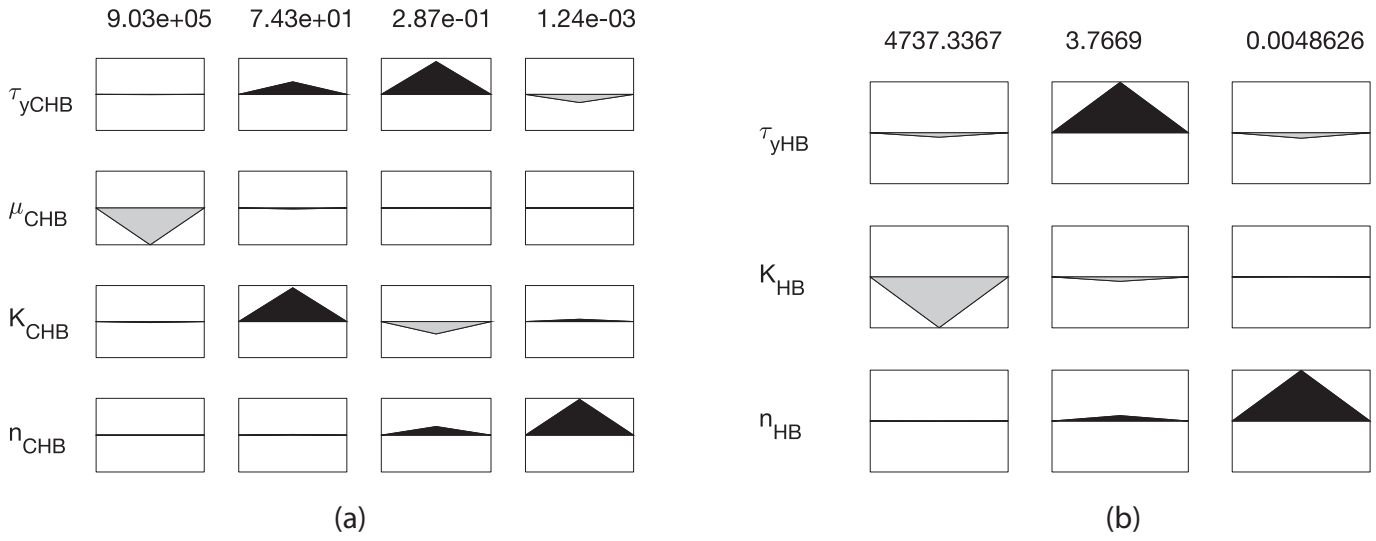

Fig. 9. Singular values and eigen vectors of the parameters for (a) CHB model and (b) HB model using rheometric data of slurry 1 at 20 °C with 11.2% TSS.

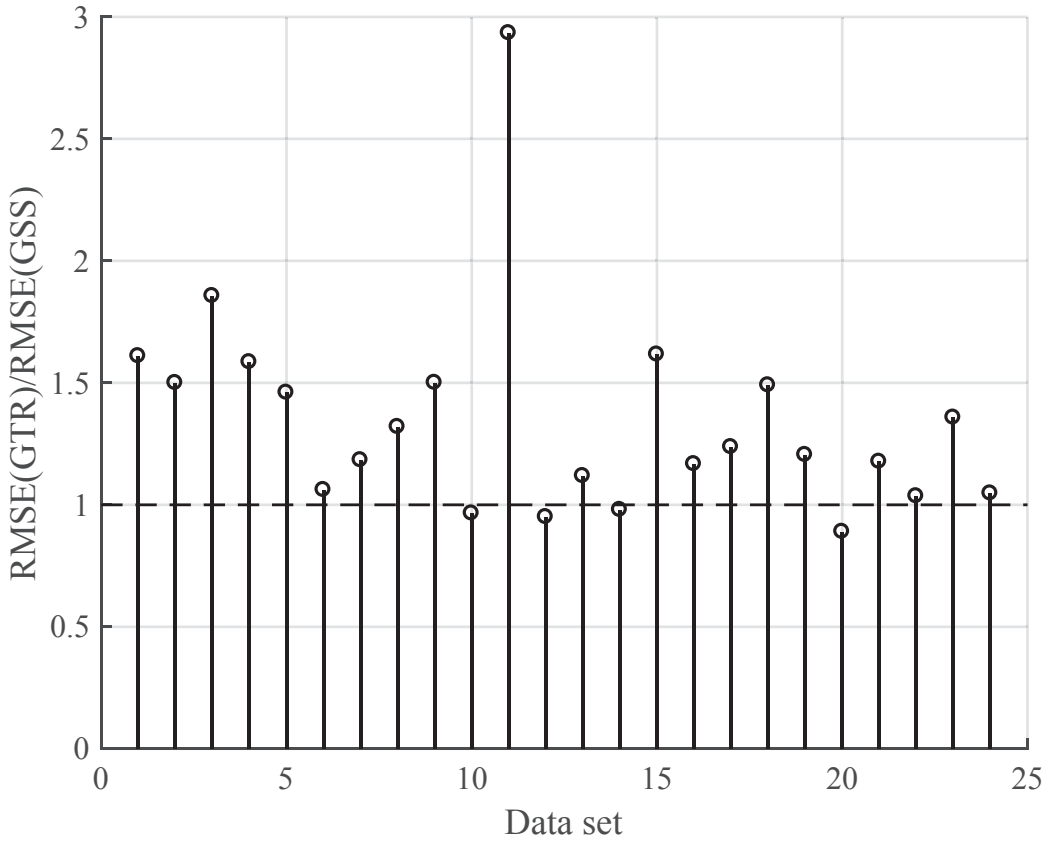

Fig. 10. Plotting the ratio of the RMSE from the algorithm GTR to the one from GSS for the data set of Slurry 1 concentration ranging 11.2 till 3.2% TSS of temperatures 10 °C, 20 °C, 30 °C, 40 °C.

$$\underline{J} = \begin{bmatrix} \frac{\partial \tau_1}{\partial \tau_{yHB}} & \frac{\partial \tau_1}{\partial K_{HB}} & \frac{\partial \tau_1}{\partial n_{HB}} \\ \vdots & \vdots & \vdots \\ \frac{\partial \tau_n}{\partial \tau_{yHB}} & \frac{\partial \tau_n}{\partial K_{HB}} & \frac{\partial \tau_n}{\partial n_{HB}} \end{bmatrix} \tag{8}$$

$$\frac{\partial \tau_n}{\partial \tau_{yHB}} = 1 \tag{9}$$

$$\frac{\partial \tau_n}{\partial K_{HB}} = \dot{\gamma}^{n_{HB}} \tag{10}$$

$$\frac{\partial \tau_n}{\partial n_{HB}} = K_{HB} n_{HB} \dot{\gamma}^{n_{HB}-1} \tag{11}$$

$$\underline{J} = \begin{bmatrix} \frac{\partial \tau_1}{\partial \tau_{yCHB}} & \frac{\partial \tau_1}{\partial \mu_{CHB}} & \frac{\partial \tau_1}{\partial K_{CHB}} & \frac{\partial \tau_1}{\partial n_{CHB}} \\ \vdots & \vdots & \vdots & \vdots \\ \frac{\partial \tau_n}{\partial \tau_{yCHB}} & \frac{\partial \tau_n}{\partial \mu_{CHB}} & \frac{\partial \tau_n}{\partial K_{CHB}} & \frac{\partial \tau_n}{\partial n_{CHB}} \end{bmatrix} \tag{12}$$

$$\frac{\partial \tau_n}{\partial \tau_{yCHB}} = 1 \tag{13}$$

$$\frac{\partial \tau_n}{\partial \mu_{CHB}} = \dot{\gamma} \tag{14}$$

$$\frac{\partial \tau_n}{\partial K_{CHB}} = \dot{\gamma}^{n_{CHB}} \tag{15}$$

$$\frac{\partial \tau_n}{\partial n_{CHB}} = K_{CHB} n_{CHB} \dot{\gamma}^{n_{CHB}-1} \tag{16}$$

$$\underline{J}^T \underline{J} = \underline{U \Sigma V} \tag{17}$$

To increase the identifiability of a unique parameter set of the HB model, in this study a method of Golden Section search (section 2.5.2) is used. This is a better algorithm in estimating the parameters for the HB model as can be seen from the RMSE ratios in Fig. 10. As this method is only applicable to the HB model, it is not applied to the entire dataset. For this, the GTR algorithm is used to identify for which of the dataset a HB model applies and then the GSS algorithm is used on these datasets.

The final estimated parameters for the models are shown in Tables 4 and 5. For the sake of representation, the HB model is used, because the HB model is a generalised model for including both the Bingham (with n = 1) and the Newtonian model (with $\tau_y = 0$ and n = 1).

3.3. Effect of concentration and temperature

Many studies have already concluded that changes in concentrations and temperature influence the rheology of the slurries to a

Table 4
Summary of the parameters estimated for the models representing the rheograms (rheometric data) of slurry 1.

Concentration	Temperature	Model	τ_y	K	n	$RMSE$
% TSS	°C	–	Pa	Pa.s^n	–	–
11.2	10	HB	1.529	0.84989	0.52	1.13E-02
	20	HB	1.398	0.82011	0.49	1.25E-02
	30	HB	1.07	0.9462	0.45	5.66E-03
	40	HB	0.855	1.38114	0.38	1.27E-02
10	10	HB	0.935	0.45995	0.55	1.45E-03
	20	HB	1.101	0.23214	0.62	5.17E-03
	30	HB	0.803	0.28666	0.56	3.76E-03
	40	HB	0.701	0.31736	0.53	2.59E-03
7.2	10	HB	0.307	0.19444	0.6	1.77E-03
	20	HB	0.444	0.06844	0.72	7.76E-04
	30	HB	0.325	0.08741	0.65	7.41E-04
	40	HB	0.372	0.06317	0.69	6.75E-04
5	10	HB	0.127	0.05864	0.69	1.01E-04
	20	HB	0.145	0.0271	0.77	4.93E-05
	30	HB	0.135	0.02123	0.78	2.25E-04
	40	HB	0.119	0.02021	0.77	2.07E-04
3.9	10	HB	0.081	0.02647	0.76	1.30E-04
	20	HB	0.076	0.01317	0.83	9.30E-05
	30	HB	0.073	0.01187	0.82	1.81E-04
	40	HB	0.02	0.02381	0.68	4.35E-04
3.2	10	HB	0.054	0.01843	0.79	1.21E-04
	20	HB	0.045	0.01057	0.85	1.26E-04
	30	HB	0.053	0.00764	0.87	1.20E-04
	40	HB	0.02	0.0133	0.75	2.68E-04
2.6	10	Bingham	0.069	0.00449	1	1.12E-04
	20	Bingham	0.053	0.00352	1	3.36E-05
	30	Bingham	0.052	0.00293	1	2.14E-05
	40	Bingham	0.047	0.00251	1	1.89E-05
1.8	10	Bingham	0.026	0.00343	1	1.33E-05
	20	Bingham	0.018	0.0027	1	4.38E-06
	30	Bingham	0.011	0.00223	1	2.49E-06
	40	Bingham	0.011	0.00186	1	3.43E-06
1.4	10	Linear	0	0.00317	1	3.61E-05
	20	Linear	0	0.00248	1	8.95E-06
	30	Linear	0	0.00204	1	1.50E-05
	40	Linear	0	0.00175	1	7.52E-06
0.7	10	Linear	0	0.00231	1	9.85E-06
	20	Linear	0	0.00182	1	1.21E-05
	30	Linear	0	0.00152	1	6.87E-06
	40	Linear	0	0.00129	1	5.80E-06
0.4	10	Linear	0	0.00195	1	3.47E-05
	20	Linear	0	0.0015	1	1.47E-05
	30	Linear	0	0.00125	1	6.73E-06
	40	Linear	0	0.00103	1	5.19E-06

Table 5
Summary of the parameters estimated for the models representing the rheograms (rheometric data) of slurry 2.

Concentration	Temperature	Model	τ_y	K	n	$RMSE$
% TSS	°C	–	Pa	Pa.s^n	–	–
3	10	HB	0.043	0.03225	0.74	0.000108
	20	HB	0.069	0.0129	0.84	0.0002
	30	HB	0.054	0.01021	0.85	0.000191
	40	HB	0.04	0.01038	0.81	0.000323
2.6	10	HB	0.048	0.0183	0.8	0.000549
	20	HB	0.043	0.00935	0.86	0.000214
	30	Bingham	0.074	0.00343	1	9.15E-05
	40	Bingham	0.057	0.00292	1	7.37E-05
2.1	10	Bingham	0.123	0.00501	1	0.000573
	20	Bingham	0.068	0.00378	1	8.70E-05
	30	Bingham	0.061	0.00303	1	3.19E-05
	40	Bingham	0.047	0.00267	1	1.77E-05
1.8	10	Bingham	0.076	0.00439	1	0.000144
	20	Bingham	0.059	0.00328	1	3.16E-05
	30	Bingham	0.044	0.00278	1	2.77E-05
	40	Bingham	0.035	0.00235	1	3.14E-05
1.2	10	Bingham	0.051	0.00375	1	6.44E-05
	20	Bingham	0.04	0.00294	1	2.11E-05
	30	Bingham	0.035	0.00244	1	7.43E-06
	40	Bingham	0.029	0.00206	1	9.06E-06
1	10	Bingham	0.042	0.00339	1	2.53E-05
	20	Bingham	0.03	0.00271	1	1.44E-05
	30	Bingham	0.023	0.00227	1	4.43E-06
	40	Bingham	0.021	0.00187	1	6.17E-06
0.8	10	Linear	0	0.00241	1	2.44E-05
	20	Linear	0	0.0019	1	1.89E-05
	30	Linear	0	0.00159	1	6.98E-06
	40	Linear	0	0.00136	1	4.92E-06

great extent (Baroutian et al., 2013; Nicky Eshtiaghi et al., 2013a, b; Mori et al., 2006; Ratkovich et al., 2013; Sanin, 2002; Seyssiecq et al., 2003). Studying the influence of temperature and concentration to the flow of the fluid i.e. rheology, is considered important, because many transportation applications and slurry handling equipment such as mixers, aerators and heat exchangers encounter gradients of temperature and concentration. These gradients may occur due to the design of such equipment or the hydrodynamic flow in them (centrifugation, settling, mixing). An interesting outcome of the rheological modelling is to breakdown the influence of concentration and temperature on the rheology to the different parameters in the model. As each parameter represents a particular phenomenon in the behaviour of the fluid flow, it is easier to understand its contribution to the flow behaviour when studied separately. The HB model will be used as a general non-Newtonian model to represent the entire range of slurry rheology.

Studying the influence of temperature and concentration through the rheological parameters imposes an extra step of caution, and this is to quantify the uncertainty in the prediction of the rheology using the parameters that have been estimated using the algorithms. What this means is that there is an inherent error presented in the model's prediction with the parameters estimated. This error represents an uncertainty band of the prediction. For the models/parameters to represent the behaviour of the slurry to the influence of temperature and concentration, the error/uncertainty bands from the model prediction must not overlap with one another. Implying that, for example investigating the influence of temperature on 10% slurry as shown in Fig. 11a, the uncertainty band of the model prediction of 10% slurry at different temperatures must not overlap. If they do, then the model parameters regressed do not represent the influence of temperature as is seen from experimental observation. Therefore, before evaluating the influence of temperature and concentration on the rheological parameters, an assessment of the uncertainty of the prediction of the models must be performed. This is to remove the uncertainty of incorrectly identifying the influence of conditions of the variables. This is done through Gauss's law of error propagation. The uncertainty in the prediction is found using Equation (19), which is for a HB model where the covariance is obtained using Equation (18).

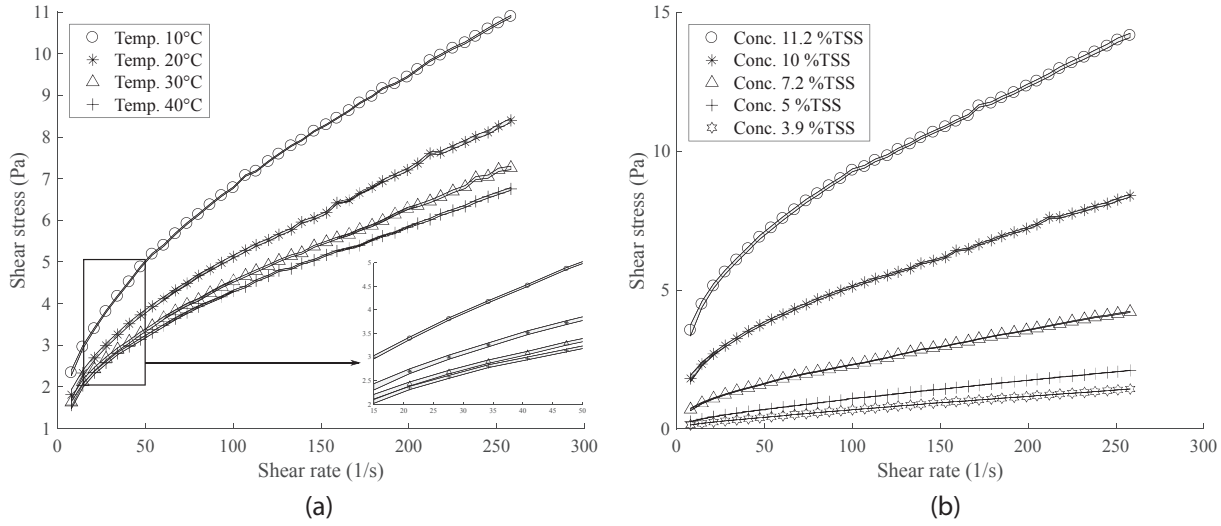

Fig. 11. Plot of the uncertainty band of the predicted values of the regressed rheological model as compared to the measure data. Plot (a) is for various temperatures of slurry 1 at 10%TSS. Plot (b) is of various concentrations of slurry 1 at 20 °C.

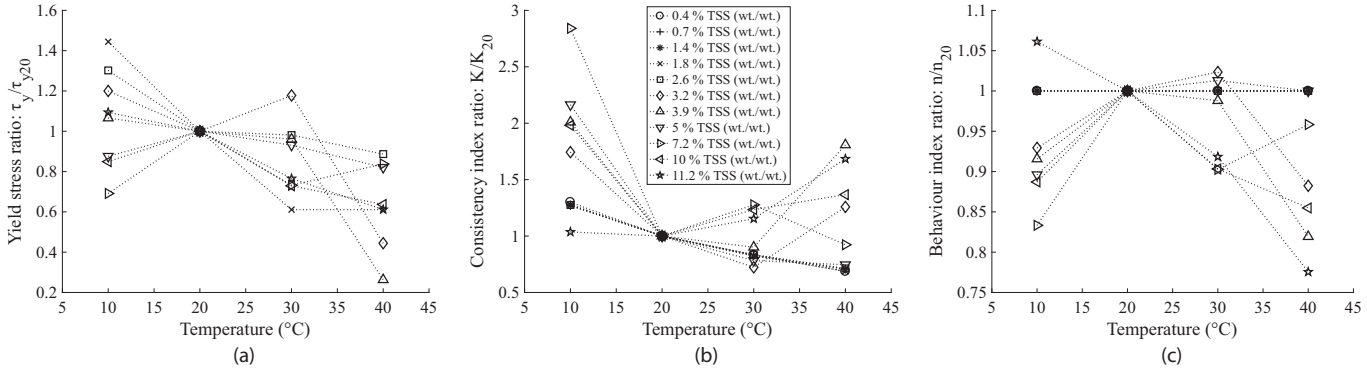

Fig. 12. Plotting the influence of temperature to the rheological parameters (a) Ratio of yield stress to the yield stress at 20 °C (b) Ratio of consistency index to the consistency index at 20 °C (c) Ratio of behaviour index to the behaviour index at 20 °C.

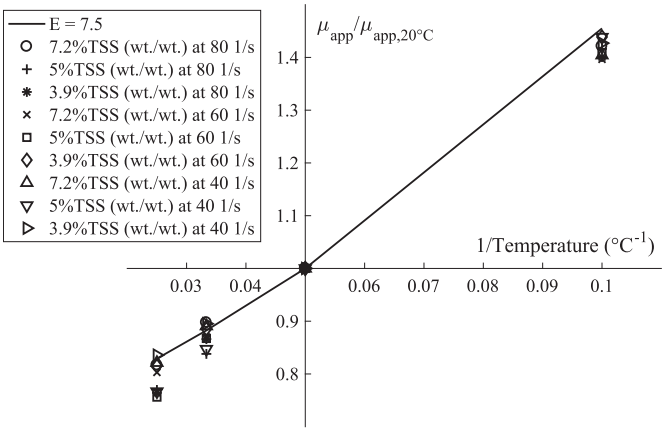

Fig. 13. Plot of apparent viscosity ratio with the inverse of temperature for different concentrations and shear rates along with the curve representing the apparent viscosity's temperature dependence with E = 7.5 (for slurry 1).

$$\textit{Covariance of Herschel} - \textit{Bulkley} = \sigma^2_{residues}\left[J^T J\right]^{-1} = \begin{bmatrix} \sigma^2_{\tau_{yHB}} & \sigma_{\tau_{yHB}}\sigma_{K_{HB}} & \sigma_{\tau_{yHB}}\sigma_{n_{HB}} \\ \sigma_{\tau_{yHB}}\sigma_{K_{HB}} & \sigma^2_{K_{HB}} & \sigma_{K_{HB}}\sigma_{n_{HB}} \\ \sigma_{\tau_{yHB}}\sigma_{n_{HB}} & \sigma_{n_{HB}}\sigma_{K_{HB}} & \sigma^2_{n_{HB}} \end{bmatrix} \tag{18}$$

$$\sigma^2_\tau = \left(\frac{\partial\tau}{\partial\tau_{yHB}}\right)^2\sigma^2_{\tau_{yHB}} + \left(\frac{\partial\tau}{\partial K_{HB}}\right)^2\sigma^2_{K_{HB}} + \left(\frac{\partial\tau}{\partial n_{HB}}\right)^2\sigma^2_{n_{HB}} + 2\left(\frac{\partial\tau}{\partial\tau_{yHB}}\right) \times \left(\frac{\partial\tau}{\partial K_{HB}}\right)\sigma_{\tau_{yHB}}\sigma_{K_{HB}} + 2\left(\frac{\partial\tau}{\partial\tau_{yHB}}\right)\left(\frac{\partial\tau}{\partial n_{HB}}\right)\sigma_{\tau_{yHB}}\sigma_{n_{HB}} + 2\left(\frac{\partial\tau}{\partial K_{HB}}\right)\left(\frac{\partial\tau}{\partial n_{HB}}\right)\sigma_{K_{HB}}\sigma_{n_{HB}} \tag{19}$$

From this, it can be observed that the uncertainty band for evaluating the effect of temperature (Fig. 11a) and concentration (Fig. 11b) do not overlap, thereby emphasizing its influence.

3.3.1. Influence of temperature

On accessing the influence of temperature on the rheological parameters (Fig. 12), no particular trend can be derived. Although from Figs. 6 and 8, it can clearly be seen that the shear stress

decreases for a given shear rate, implying that the viscosity decreases with temperature, the same does not reflect on the individual parameters. For this reason, the influence of the temperature on the rheology is resolved through its effect on the apparent viscosity. An Arrhenius type equation (Abu-Jdayil et al., 2010; Battistoni et al., 1993; Pevere et al., 2009; Yang et al., 2009) is used for this purpose. The apparent viscosity (Ratio of shear-stress by shear-rate at a shear-rate) can be described using equation (20) as a function of temperature, where a and E are constants.

$$\mu_{app} = ae^{E/T} \tag{20}$$

On taking the ratio of the apparent viscosities at two different temperatures, we get equation (21), which is independent of the constant a. Implying, if the apparent viscosity at a particular temperature is known, with the knowledge of E (rheological temperature constant, °C), the apparent viscosity at another temperature can be calculated.

$$\frac{\mu_{app,\,T_1}}{\mu_{app,T_2}} = e^{E\left(\frac{1}{T_1}-\frac{1}{T_2}\right)} \tag{21}$$

Accessing the value of E for apparent viscosity ratios at various concentrations and shear rates, an average value of 7.5 °C was obtained (Fig. 13), and this holds good for slurry 1 and slurry 2. Knowing the value of E is useful, as in the following sections parameter models are introduced for the slurry at 20 °C, and to obtain the rheology at other temperatures, this rheological temperature constant can be used.

3.3.2. Yield stress τ_y

The yield stress specifies the minimum stress that is required for the slurry to start flowing, below which it can impede the flow. Over the range of concentrations, the yield stress increases exponentially as illustrated in Fig. 14. There is a pronounced exponential behaviour in slurry 1. Whereas in slurry 2 an underlying behaviour is not identified, this could be that the sample size is small and at low concentrations. An exponential model (Fig. 15a, equation (22), <5% deviation from the measurements) is used describe the influence of concentration on yield stress of slurry 1 at 20 °C (chosen as a representative), this model type has been reportedly used in other works (Eshtiaghi et al., 2013a, b; Seyssiecq et al., 2003). It can be seen that the yield stress is effectively 0 below a threshold concentration, and then increases above this concentration. The exponential behaviour in Slurry 1 can be explained through the increase in particle interactions as the concentration increases. These interactions are weak physical forces between particles and molecules. Although these forces are weak, with the increase in concentrations the number of neighbouring particles in interaction increase and thus creating a structure. The yield stress tends to zero at low concentrations and is physically meaningful only after reaching a certain concentration (also observed in equation (22), a threshold concentration), where its effects can be felt. For our case

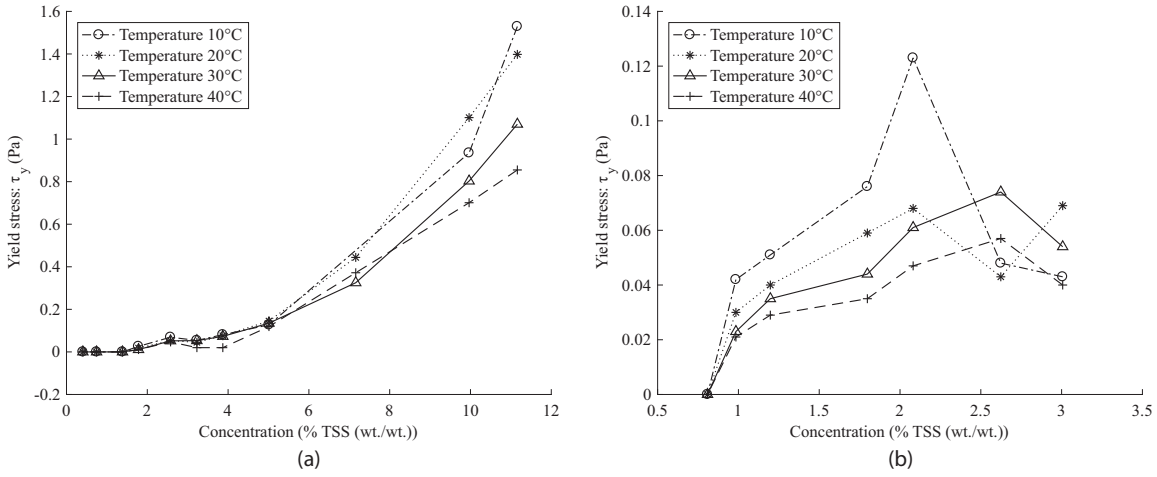

Fig. 14. Change of yield stress τ_y with concentration and temperature in (a) slurry 1 and (b) slurry 2.

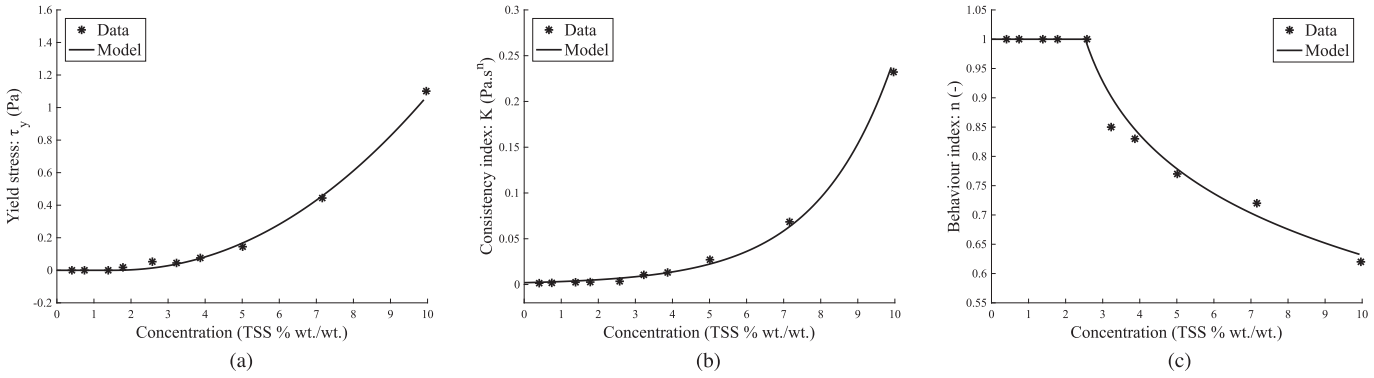

Fig. 15. Models representing the influence of concentration on (a) yield stress (b) consistency index (c) behaviour index for slurry 1 at 20 °C.

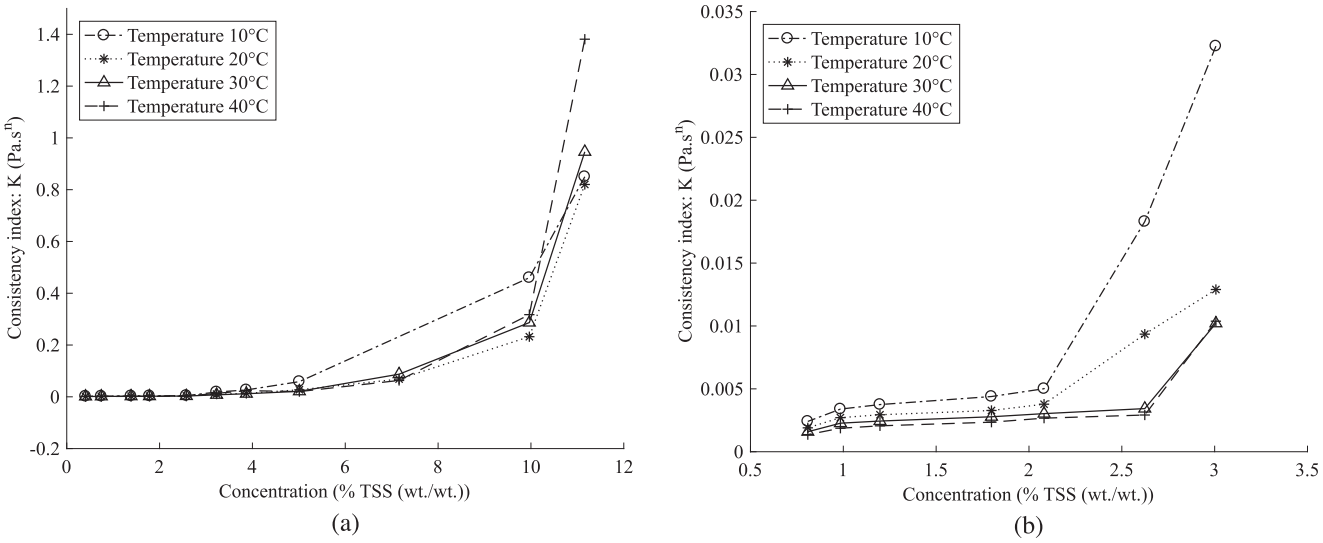

Fig. 16. Change of consistency index K with concentration and temperature in (a) slurry 1 and (b) slurry 2.

of Slurry 1 this is 1.5 %TSS.

$$\begin{array}{ll} \tau_y = 0.012\ (C - 1.5)^{2.1} & \text{for C} > 1.5\,\%\ \text{TSS (wt./wt.)} \\ \tau_y = 0 & \text{for C} < 1.5\,\%\ \text{TSS (wt./wt.)} \end{array} \quad (22)$$

3.3.3. Consistency index ***K***

The consistency index gives an idea about the viscosity of the slurry. Although, both the τ_y and n are required to compute the absolute viscosity, K can be used to perceive the viscous behaviour of the slurry. Over the range of concentrations, the consistency index exponentially increases (Fig. 16). As a representative, equation (23) (derived with <5% deviation) describes the concentration dependence of the consistency index of slurry 1 at 20 °C (Fig. 15b). It takes the value of the viscosity of water at 0%TSS of the slurry. The exponential increase of the flow index is observed in both slurry 1 and 2 clearly. The observed behaviour, which is similar to the yield stress, can also be attributed to the forces between the constituent particles.

$$K = 0.002e^{0.48\ C} \quad (23)$$

3.3.4. Behaviour index ***n***

The behaviour index describes the shear thinning behaviour of the slurry. This is an important parameter as it governs the influence of the change in shear-rate on the shear-stress. Newtonian fluids have the behaviour index as 1, meaning that an increase in shear-rate increases the shear-stress proportional to the consistency index. But with non-Newtonian Fluids with the behaviour index less than 1 implies that a change in shear-rate might not necessarily reflect in a sizeable change in the shear-stress even though the consistency index has a high value. This is essentially the shear thinning behaviour observed in these slurries. As a representative, equation (24) (derived with <5% deviation) describes the behaviour index as a function of concentration for slurry 1 at 20 °C (Fig. 15c). Over the range of concentrations, the onset of shear-thinning behaviour is at a concentration of 2.5%TSS. Above this concentration, the behaviour index decreases gradually with the concentration of the slurry (Fig. 17). This behaviour may be a reflection of the fluid structures, referred to by Quemada (1998) as a structural unit, SU, introducing the concept of effective volume fraction of the SUs as a basis for rheological models. The shear thinning behaviour occurs with the breakup of fluid structures and the constituent particles aligning in the direction of the flow. At low shear-rates, there isn't enough shearing to breakup these fluid structures, but as the shearing rate increases more fluid structures are broken and the constituent particles align with the flow, thereby making it easier to flow, i.e. shear thinning. The increase in

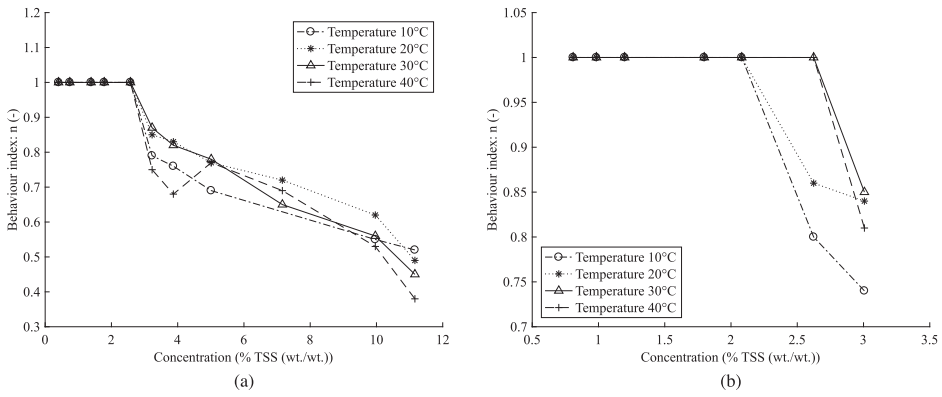

Fig. 17. Change of behaviour index n with concentration and temperature in (a) slurry 1 and (b) slurry 2.

concentration causes an increase in fluid structures present and by that the proportion of fluid structures broken is higher, i.e. increased shear thinning.

$$\begin{aligned} n &= 0.97 - 0.16\log(C - 1.7) \quad \text{for C} > 2.5\ \%\ \text{TSS (wt./wt.)} \\ n &= 1 \qquad\qquad\qquad\qquad\quad \text{for C} < 2.5\ \%\ \text{TSS (wt./wt.)} \end{aligned} \tag{24}$$

3.4. Effect of adding kitchen waste

Comparing the viscosities of both the slurries, it is observed that the viscosity of slurry 2 is on an average (approximate averaging: over all concentration and 3 different shear-rates) 50% more than that of slurry 1 (Fig. 18). This could be explained by comparing the particle size distribution of both slurries (Fig. 3). Slurry 2 has a higher D90 than that of slurry 1 (section 2.1). Adding to this, the proportion of larger particles is higher in slurry 2 than in slurry 1 (Fig. 3) signifying that the particle size distribution of kitchen waste tends towards larger particles. Therefore, this affirms that the particle size distribution plays a major role in determining the viscosities of slurries of this nature. That being said, the sample collected here is small to put forth a strong conclusion about the addition of kitchen waste. Further research could shed light on these aspects.

3.5. Comparison with waste-water treatment plant sludge

A select few of the available literature data is compared with the slurries studied in this paper. Primary and secondary sludge from (Markis et al., 2014), and anaerobic digested sludge from (Baudez et al., 2011) is compared. In comparison to the waste-water treatment plant (WWTP) sludge, the CDS behaves similarly with respect to the non-Newtonian characteristics (Fig. 19). At low concentrations, the non-Newtonian behaviour is predominantly that of Bingham type, with a low yield stress. This can be seen for Slurry 1 with 5% TSS (wt./wt.), Primary sludge 2.8% TSS (wt./wt.) and Anaerobic digested sludge at 1.8% TSS (wt./wt.). As the concentration of suspended solids increase, the shear thinning behaviour comes into play with a higher yield stress. Therefore, leading to a Herschel-Bulkley type behaviour. Slurry 1 at 11.2% TSS (wt./wt.) and secondary sludge at 3.7% TSS (wt./wt.) show similar Herschel-Bulkley behaviour.

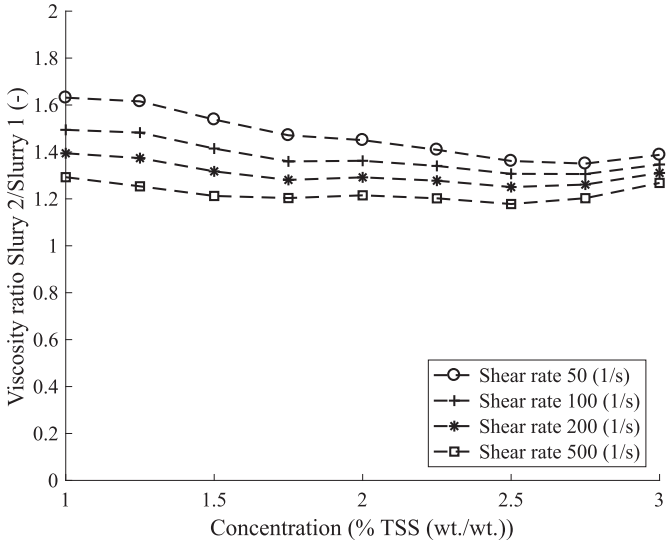

Fig. 18. Plot of viscosity ratio between Slurry 1 and 2 against TSS concentration at different shear rates.

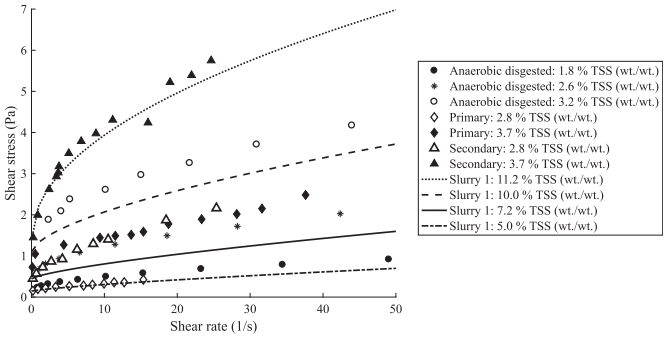

Fig. 19. Comparing rheograms of slurry 1 with primary and secondary sludge from (Markis et al., 2014) and anaerobic digested sludge from (Baudez et al., 2011).

4. Conclusion

To study the hydrodynamic behaviour of concentrated domestic slurries, 2 sample slurries from a pilot project involving novel sanitations systems were collected. Slurry 1 contained black water and slurry 2 black water with ground kitchen waste. These samples were later processed and studied for their rheology using a narrow gap couette rheometer chosen appropriately for their particle size distribution. Rheograms were obtained for various TSS concentration and temperatures of slurries. Among the rheological models explored, the Herschel-Bulkley (HB) model fits best the purpose of describing the obtained rheograms. In general, the viscosity increases with increase in TSS concentration and decreases with increase in temperature; and this reflects on the parameters. To describe the effect of temperature on the rheology of the slurry, an Arrhenius type equation is used. The influence of concentration on the rheology is described using the changes in these parameters. The yield stress and consistency index are exponentially related to the concentration, whereas the behaviour index has a decreasing power law relation. Comparing the viscosities of slurry 1 and 2, reveals that the addition of kitchen waste increases the viscosity. The knowledge on the rheology thus collected can be used to predict the pressure drop in the transport of CDS and thus can be used to evaluate and design different sanitation options.

Acknowledgement

This project is carried out by Delft University of Technology and funded by Technology Foundation STW under the grant number 13347 with the user committee of Deltares, Stowa, stichting RIONED, Waternet, Waterboard Zuiderzeeland, Sweco and XYLEM.

References

Abu-Jdayil, B., Banat, F., Al-Sameraiy, M., 2010. Steady rheological properties of rotating biological contactor (RBC) sludge. J. Water Resour. Prot. 2, 1–7.
Ashley, R.M., Bertrand-Krajewski, J.L., Hvitved-Jacobsen, T., Verbanck, M., 2005. Solids in sewers: characteristics, effects and control of sewer solids and associated pollutants. Water Intell. Online 4, 9781780402727.
Association, A.P.H., 2005. Standard Methods for the Examination of Water and Wastewater. American Public Health Association (APHA), Washington, DC, USA.
Baroutian, S., Eshtiaghi, N., Gapes, D.J., 2013. Rheology of a primary and secondary sewage sludge mixture: dependency on temperature and solid concentration. Bioresour. Technol. 140, 227–233.
Battistoni, P., Fava, G., Stanzini, C., Cecchi, F., Bassetti, A., 1993. Feed characteristics and digester operative conditions as parameters affecting the rheology of digested municipal solid wastes. Water Sci. Technol. 27, 37–45.
Baudez, J.C., Markis, F., Eshtiaghi, N., Slatter, P., 2011. The rheological behaviour of anaerobic digested sludge. Water Res. 45, 5675–5680.
Baudez, J.C., Slatter, P., Eshtiaghi, N., 2013. The impact of temperature on the

rheological behaviour of anaerobic digested sludge. Chem. Eng. J. 215, 182–187.
Braun, R., Wellinger, A. (Eds.), 2003. Potential of Co-digestion. IEA Bioenergy, Task.
Byrd, R.H., Schnabel, R.B., Shultz, G.A., 1987. A trust region algorithm for nonlinearly constrained optimization. SIAM J. Numer. Anal. 24, 1152–1170.
Chaudhuri, A., Wereley, N.M., Radhakrishnan, R., Choi, S.B., 2006. Rheological parameter estimation for a ferrous nanoparticle-based magnetorheological fluid using genetic algorithms. J. Intell. Mater. Syst. Struct. 17, 261–269.
Chilton, R., Stainsby, R., Thompson, S., 1996. The design of sewage sludge pumping systems. J. Hydraul. Res. 34, 395–408.
Eshtiaghi, N., Baudez, J., Slatter, P., 2013a. Rheological behaviour of anaerobic digested sludge: impact of concentration and temperature. In: AD 13: Recovering (Bio) Resources for the World. International Water Association (IWA), pp. 1–4.
Eshtiaghi, N., Markis, F., Slatter, P., 2012. The laminar/turbulent transition in a sludge pipeline. Water Sci. Technol. 65, 697–702.
Eshtiaghi, N., Markis, F., Yap, S.D., Baudez, J.-C., Slatter, P., 2013b. Rheological characterisation of municipal sludge: a review. Water Res. 47, 5493–5510.
Hager, W.H., 2010. Wastewater Hydraulics: Theory and Practice. Springer Science & Business Media.
Iacovidou, E., Ohandja, D.-G., Gronow, J., Voulvoulis, N., 2012a. The household use of food waste disposal units as a waste management option: a review. Crit. Rev. Environ. Sci. Technol. 42, 1485–1508.
Iacovidou, E., Ohandja, D.-G., Voulvoulis, N., 2012b. Food waste co-digestion with sewage sludge–realising its potential in the UK. J. Environ. Manag. 112, 267–274.
Kelessidis, V.C., Maglione, R., Tsamantaki, C., Aspirtakis, Y., 2006. Optimal determination of rheological parameters for Herschel–Bulkley drilling fluids and impact on pressure drop, velocity profiles and penetration rates during drilling. J. Pet. Sci. Eng. 53, 203–224.
Kujawa-Roeleveld, K., Elmitwalli, T., Zeeman, G., 2006. Enhanced primary treatment of concentrated black water and kitchen residues within DESAR concept using two types of anaerobic digesters. Water Sci. Technol. 53, 159–168.
Larsen, T.A., Alder, A.C., Eggen, R.I.L., Maurer, M., Lienert, J., 2009. Source separation: will we see a paradigm shift in wastewater handling? Environ. Sci. Technol. 43, 6121–6125.
Lundie, S., Peters, G.M., 2005. Life cycle assessment of food waste management options. J. Clean. Prod. 13, 275–286.
Markis, F., Baudez, J.-C., Parthasarathy, R., Slatter, P., Eshtiaghi, N., 2014. Rheological characterisation of primary and secondary sludge: impact of solids concentration. Chem. Eng. J. 253, 526–537.
Mori, M., Seyssiecq, I., Roche, N., 2006. Rheological measurements of sewage sludge for various solids concentrations and geometry. Process Biochem. 41, 1656–1662.
Nakakubo, T., Tokai, A., Ohno, K., 2012. Comparative assessment of technological systems for recycling sludge and food waste aimed at greenhouse gas emissions reduction and phosphorus recovery. J. Clean. Prod. 32, 157–172.
Ohen, H.A., Blick, E.F., 1990. Golden section search method for determining parameters in Robertson-Stiff non-Newtonian fluid model. J. Pet. Sci. Eng. 4, 309–316.
Pevere, A., Guibaud, G., Goin, E., Van Hullebusch, E., Lens, P., 2009. Effects of physico-chemical factors on the viscosity evolution of anaerobic granular sludge. Biochem. Eng. J. 43, 231–238.
Quemada, D., 1998. Rheological modelling of complex fluids. I. The concept of effective volume fraction revisited. Eur. Phys. J. Appl. Phys. 1, 119–127.
Ratkovich, N., Horn, W., Helmus, F.P., Rosenberger, S., Naessens, W., Nopens, I., Bentzen, T.R., 2013. Activated sludge rheology: a critical review on data collection and modelling. Water Res. 47, 463–482.
Rooki, R., Ardejani, F.D., Moradzadeh, A., Mirzaei, H., Kelessidis, V., Maglione, R., Norouzi, M., 2012. Optimal determination of rheological parameters for herschel-bulkley drilling fluids using genetic algorithms (GAs). Korea Aust. Rheol. J. 24, 163–170.
Sanin, D.F., 2002. Effect of solution physical chemistry on the rheological properties of activated sludge. Water SA 28, 207–212.
Seyssiecq, I., Ferrasse, J.-H., Roche, N., 2003. State-of-the-art: rheological characterisation of wastewater treatment sludge. Biochem. Eng. J. 16, 41–56.
Slatter, P.T., 1997. The rheological characterisation of sludges. Water Sci. Technol. 36, 9–18.
Slatter, P.T., Thomas, P., 1995. Transitional and Turbulent Flow of Non-Newtonian Slurries in Pipes.
Tervahauta, T., Hoang, T., Hernández, L., Zeeman, G., Buisman, C., 2013. Prospects of Source-Separation-Based sanitation concepts: a model-based study. Water 5, 1006–1035.
Thomas, A.D., Wilson, K.C., 1987. New analysis of non-Newtonian turbulent flowndashyield-power-law fluids. Can. J. Chem. Eng. 65, 335–338. https://doi.org/10.1002/cjce.5450650221.
Thota Radhakrishnan, A., Alidai, A., Pothof, I., van Lier, J., Clemens, F., 2015. Predicting the onset of secondary flows in the rheological measurement of domestic slurry. In: 10th International Conference on Urban Drainage Modelling.
Van Wazer, J.R., 1963. Viscosity and Flow Measurement: a Laboratory Handbook of Rheology. Interscience Publishers.
Woolley, S.M., Cottingham, R.S., Pocock, J., Buckley, C.A., 2014. Shear rheological properties of fresh human faeces with different moisture content. Water SA 40, 273–276.
Yang, F., Bick, A., Shandalov, S., Brenner, A., Oron, G., 2009. Yield stress and rheological characteristics of activated sludge in an airlift membrane bioreactor. J. Membr. Sci. 334, 83–90.
Zeeman, G., Kujawa, K., Mes, T. de, Hernandez, L., Graaff, M. de, Abu-Ghunmi, L., Mels, A., Meulman, B., Temmink, H., Buisman, C., 2008. Anaerobic treatment as a core technology for energy, nutrients and water recovery from source-separated domestic waste (water). Water Sci. Technol. 57, 1207–1212.